Radiation Physics and Chemistry 81 (2012) 1600–1605

Contents lists available at SciVerse ScienceDirect

Radiation Physics and Chemistry

journal homepage: www.elsevier.com/locate/radphyschem

Irradiation effects of 6 MeV electron on electrical properties of Al/Al_2O_3/n-Si MOS capacitors

P. Laha[a], I. Banerjee[a,d], A. Bajaj[a], P. Chakraborty[e], P.K. Barhai[a], S.S. Dahiwale[f], A.K. Das[b], V.N. Bhoraskar[c], D. Kim[f], S.K. Mahapatra[a,*]

[a] Department of Applied Physics, Birla Institute of Technology, Mesra, Ranchi 835215, India
[b] Laser & Plasma Technology Division, Bhabha Atomic Research Center, Mumbai 400085, India
[c] Department of Physics, University of Pune, Pune 411007, India
[d] Department of Mechanical and Aerospace Engineering, University of California, Los Angeles, CA 90095, USA
[e] Saha Institute of Nuclear Physics, I/AF, Bidhannagar, Kolkata-700064, India
[f] Department of Material Science and Engineering, Korea University, Seoul, Republic of Korea

ARTICLE INFO

Article history:
Received 6 September 2011
Accepted 12 April 2012
Available online 21 April 2012

Keywords:
MOS device
Electron irradiation
Interface trap density
Flat band voltage
Leakage current
Al_2O_3

ABSTRACT

The influence of 6 MeV electron irradiation on the electrical properties of Al/Al_2O_3/n-Si metal–oxide–semiconductor (MOS) capacitors has been investigated. Using rf magnetron sputtering deposition technique, Al/Al_2O_3/n-Si MOS capacitors were fabricated and such twelve capacitors were divided into four groups. The first group of MOS capacitors was not irradiated with 6 MeV electrons and treated as virgin. The second group, third group and fourth group of MOS capacitors were irradiated with 6 MeV electrons at 10 kGy, 20 kGy, and 30 kGy doses, respectively, keeping the dose rate ~1 kGy/min. The variations in crystallinity of the virgin and irradiated MOS capacitors have been compared from GIXRD (Grazing Incidence X-ray Diffraction) spectra. Thickness and in-depth elemental distributions of individual layers were performed using Secondary Ion Mass Spectrometry (SIMS). The device parameters like flat band voltage (V_{FB}) and interface trap density (D_{it}) of virgin and irradiated MOS capacitors have been calculated from C vs V and G/ω vs V curve, respectively. The electrical properties of the capacitors were investigated from the tan δ vs V graph. The device parameters were estimated using C–V and G/ω–V measurements. Poole–Frenkel coefficient (β_{PF}) of the MOS capacitors was determined from leakage current (I)–voltage (V) measurement. The leakage current mechanism was proposed from the β_{PF} value.

1. Introduction

In the last few decades, the studies related to the design and characterization of the MOS device has been carried out for its better performance (Xuan et al., 2006). The focuses of several studies are on dependence of MOS parameters in thickness, dielectric constant, grain size and crystallinity of the oxide materials (Voigt and Sokolowski, 2004; Bhuvaneswari et al., 2006). Although, the fabrication of MOS device can be tailored by different methods to make it suitable for required applications where as the development of such radiation hardened MOS device is still challenging (García et al., 2009).

During the mission period in the geostationary earth orbit or lower earth orbit, the outer surfaces of the satellite get exposed to different types of space radiations like keV to MeV energy electrons, heavy ions and eV energy oxygen atoms (Popov et al., 1997; McKenna-Lawlor et al., 2003). The keV electrons produce a few kV on the outer surface of the satellite and therefore it can exceed the voltage sufficient to initiate the spacecraft charging, which produces leakage current in the devices used in the satellite (Frederickson, 1993; Garrett and Whittlesey, 2000). However, the high energy electrons can penetrate the satellite surface and interact with the electronic devices. The high energy electron interacts with the oxide layers of MOS devices and creates electron–hole pairs which are proportional to the radiation dose (Enge, 1972). Some fraction of this electron–hole pairs recombine in the oxide layer and remaining electron–hole pairs escaping out of it. This recombination produce ionization damage in the form of oxide traps and interface traps (Kim et al., 2004). Hence, the high energetic particles also cause degradation and failure of the electronic, electrical systems and catastrophic failure in space vehicles or satellites (Schmidt et al., 1969; Cricchi and Barbe, 1971; Kim et al., 2004). Although, the effects

* Corresponding author. Department of Physics and Astronomy, University of California, Los Angeles, CA 90095, USA
E-mail addresses: skm@physics.ucla.edu, skmahapatra@bitmesra.ac.in (S.K. Mahapatra).

0969-806X/$ - see front matter © 2012 Elsevier Ltd. All rights reserved.
http://dx.doi.org/10.1016/j.radphyschem.2012.04.006

of ionizing radiation on MOS devices have been studied extensively since 1960s using electron beam irradiation (Winokur et al., 1984), reports related to irradiation effects on electrical properties of the MOS capacitor are in scarce. One of the solutions to reduce the disastrous effects of the radiation is to modify the oxide materials in the MOS structure in such a way that the required device parameters can be realized (Tuğluoğlua et al., 2004) at radiation environment. Therefore, the study of radiation effects on the oxide materials for MOS device has gained importance for the space applications.

The radiation hardened MOS device, demands for wide band gap, high effective dielectric constant and thermally stable material (Soliman et al., 1995; Hughes and Benedetto, 2003). Conventionally, SiO_2 is used in MOS capacitors for radiation enriched space environment but Al_2O_3 could be better alternative of SiO_2 due to its large band gap of E_g=8.8 eV, dielectric constant ~8–10, band offset to Si and thermal stability. In view of this, Al_2O_3 may be a good substitute of SiO_2 and needs further investigation for radiation hardened MOS device (Soliman et al., 1995). A few reports are available on electron irradiation effect on MOS capacitor but a systematic study is required to correlate the radiation dose with leakage current and device parameters.

In this paper, Al/Al_2O_3/n-Si capacitors were fabricated using rf reactive magnetron sputtering system. The capacitors were post irradiated with 6 MeV electrons at different doses; (a) zero (virgin), (b) 10 kGy, (c) 20 kGy, and (d) 30 kGy. The device parameters were estimated using C–V and G/ω–V measurements, and the leakage current mechanism was proposed from the ln $|J|$ vs $\sqrt{E}$ plots. The effect of electron irradiation was found to cause permanent changes in the silicon crystallinity, interfacial dangling bonds, defects and charge trapping in the MOS capacitor. The flat band voltage of irradiated Al/Al_2O_3/n-Si capacitor has been compared with reported data.

2. Experimental details

To fabricate the MOS capacitors, silicon substrates, of size 10 mm × 10 mm × 0.5 mm, were obtained by cutting n type silicon wafers. These substrates were initially cleaned by the dilute HF acid, rinsed with deionized water and dried at room temperature. The rf magnetron sputtering system was used for thin film coating of Al_2O_3 and aluminum on the silicon substrates. The details of the rf magnetron sputtering deposition system, along with the vacuum pumps, etc., were provided in our previous publication (Laha et al., 2010). The aluminum (99.99%) sputter target of 50 mm diameter and 3 mm thickness was used. After mounting a few n type Si substrates on the sample holder inside the deposition chamber, the deposition chamber was evacuated to obtain a base pressure of $\sim 10^{-6}$ mbar. The aluminum targets were cleaned by the sputtering method, using argon gas. The argon and oxygen gases were inserted inside the chamber, at equal flow rate of ~50 sccm each with maintaining working pressure $\sim 6 \times 10^{-2}$ mbar at rf power of 100 W.

Initially, using the aluminum target, aluminum oxide thin films of different thicknesses were deposited on silicon substrates, by varying sputtering period from 3 to 21 min, in a step of 3 min. The structure and the thickness of each aluminum oxide film deposited on n type silicon substrates were studied, respectively, by GIXRD (Grazing Incidence X-ray Diffraction) and Ellipsometry methods. From the plot of the film thickness and period of deposition, the rf sputtering system could be calibrated. The GIXRD results confirmed that the deposited film had Al_2O_3 structure. For a sputtering period of 15 min, the deposited film was found to be uniform, with high degree of Al_2O_3 structure. Later on, thin film of Al_2O_3 of thickness 100 nm was deposited on a number of silicon substrates, by keeping the deposition time of 15 min. After that, using the aluminum target, thin film of aluminum of thickness 275 nm, was deposited on each of the Al_2O_3 coatings, by keeping deposition time of 7 min. In this manner, Al/Al_2O_3/n-Si MOS capacitors were fabricated in the laboratory.

All these laboratory made Al/Al_2O_3/n-Si MOS capacitors were characterized by (i) Ellipsometer (Nano-View Inc., Korea; SEMG1000-VIS) for the measurement of the layer thickness, (ii) SIMS (Model: Hiden, UK) for in depth elemental analysis, (iii) GIXRD (Model: PAN analytical X' Pertpro 3040/60) for measurement of crystallographic structure, (iv) C–V, G/ω–V and tan δ–V (HP4284 LCR Meter) for the estimation of device parameters, and (v) current–voltage (2410 Keithley Source meter) measurement for leakage current study.

The characterized MOS capacitors were divided into four groups, each consisting of three capacitors. These capacitors were irradiated with 6 MeV electrons. The 6 MeV electrons beam, of pulse width ~1.6 μs, had diameter ~3 mm after exiting from the extraction window of Microtron. The electron beam was therefore scattered by a thin tungsten foil, to cover the entire area (10×10 mm^2) of the capacitor. For irradiation experiment, one capacitor at a time was mounted on the Faraday cup, placed at a distance of ~150 mm away from the extraction port in air. The Faraday cup was connected to a current integrator for measuring the number of electrons falling on the capacitor. In this manner, each capacitor of the first group was irradiated with 6 MeV electrons to a dose of 10 kGy. Similarly, capacitors of the second and the third groups were irradiated with 6 MeV electrons to doses of 20 kGy and 30 kGy, respectively. All the capacitors were irradiated at a constant dose rate ~1 kGy/min. All the electron irradiated capacitors were also characterized following the same procedures as that adopted for the as prepared capacitors.

3. Results and discussions

The laboratory made Al/Al_2O_3/n-Si MOS capacitors were divided into four groups. The first group of capacitor was kept as virgin and coded by "a". The second group was irradiated with 6 MeV electrons at 10 kGy dose and coded by "b". Similarly, the third and the forth groups were irradiated with 6 MeV electrons at 20 kGy, 30 kGy and coded by "c" and "d", respectively. The elemental concentrations of each layer of only sample a

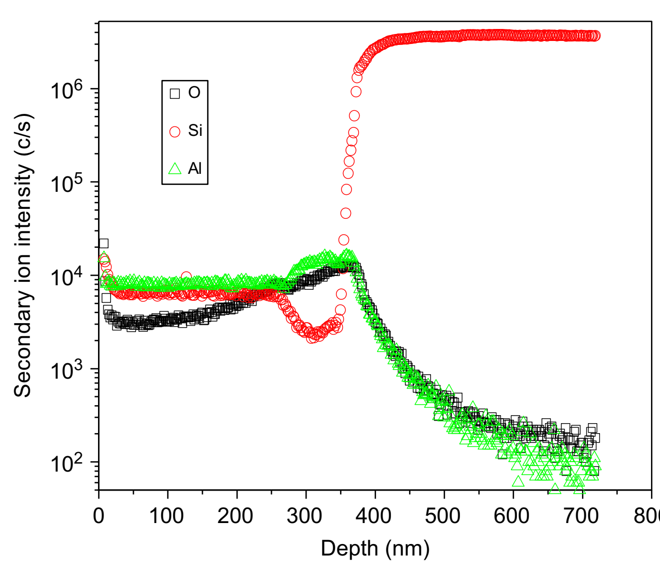

Fig. 1. SIMS depth profiles of virgin laboratory made Al/Al_2O_3/n-Si, a MOS capacitor.

(laboratory made capacitor) were characterized by SIMS technique whereas, the crystallinity of each samples a–d was studied by GIXRD technique. The results of SIMS and GIXRD are shown in Figs. 1 and 2, respectively. Similarly the device parameters of each samples a–d are shown in Table 1 and also explained by Figs. 3–8.

Fig. 1 shows the SIMS depth profiles of virgin Al/Al_2O_3/n-Si MOS structure which is denoted by sample "a". As seen in the figure, the measured oxide film (Al_2O_3) thickness is ~100 nm. The thickness of the Al cap layer for all samples as measured through SIMS is ~275 nm. The sharp rise of Si and fall off of Al and O signals at around the same region signifies the film/substrate interface positions. Extended declining trend of Al and O signals beyond the film/substrate interface indicates an appreciable inter-diffusion of these two elements and the Si substrate. For sample "a", the beginning of the small hump of Al signal indicates the position of Al/Al_2O_3 interface and it signifies the presence of Al_2O_3 interlayer. The monotonic rise of oxygen extending up to Al_2O_3/Si substrate region followed by a subsequent steady decline confirms that oxygen has inter diffused across the entire multilayer stack. Similarly, the physical thickness of the Al and Al_2O_3 layers were measured through ellipsometry. The obtained Al and Al_2O_3 thickness are found to be in close agreement with the SIMS thickness of ~275 nm and ~100 nm, respectively.

Fig. 2 shows the GIXRD spectra of samples a–d. Fig. 2(a) show peaks at $2\theta=43.01^\circ$ and 51.75° corresponding to the plane (1 1 3) of Al_2O_3 (JCPDS card No.81-1468) and (2 3 0) plane of $Al_2(SiO_4)O$ (JCPDS card No.87-1712). Fig. 2(b)–(d) show peaks at $2\theta=23.08^\circ$, 32.78°, 43.01° and 51.75° corresponding to (1 1 1) plane of $Al_2(SiO_4)O$ (JCPDS card No.87-1712), (0 0 2) plane of Al_2O_3 (JCPDS card No.86-1410), (1 1 3) plane of Al_2O_3 (JCPDS card No.82-1468)

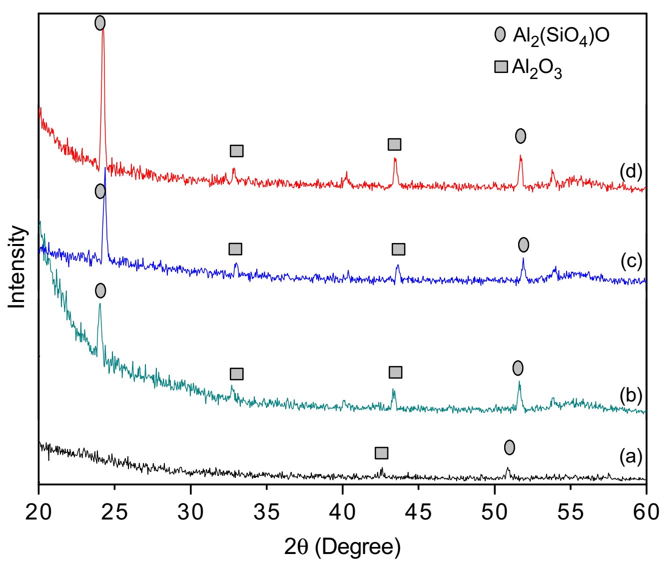

Fig. 2. GIXRD spectra of Al_2O_3 thin film of Al/Al_2O_3/n-Si MOS capacitors with different electron radiation doses. (i) Zero, a, (ii) 10 kGy, b, (iii) 20 kGy, c, and (iv) 30 kGy, d.

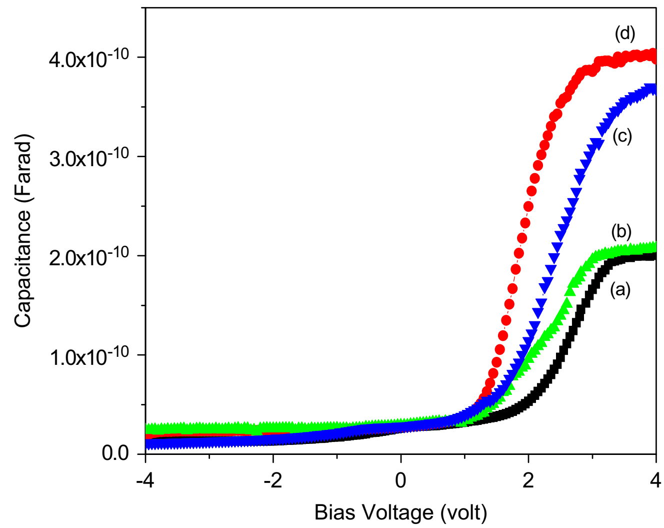

Fig. 3. *C–V* characteristic of Al/Al_2O_3/n-Si MOS capacitors with different electron radiation doses. (i) Zero, a, (ii) 10 kGy, b, (iii) 20 kGy, c, and (iv) 30 kGy, d.

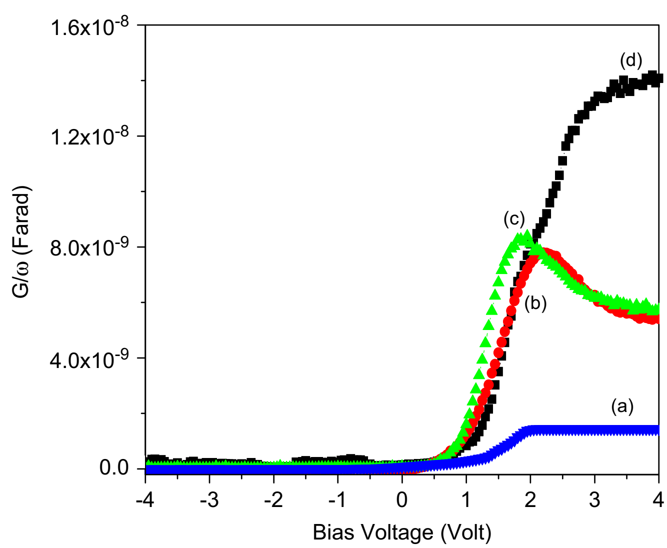

Fig. 4. *G/ω–V* characteristic of Al/Al_2O_3/n-Si MOS capacitors with different electron radiation doses. (i) Zero, a, (ii) 10 kGy, b, (iii) 20 kGy, c, and (iv) 30 kGy, (d).

Table 1
Variations in C_{OX}, V_{FB}, $(G/\omega)_{max}$, tan δ peak, D_{it} and conduction mechanism of laboratory made Al/Al_2O_3/n-Si MOS capacitors irradiated with 6 MeV electrons at different doses. (i) Zero, a, (ii) 10 kGy, b, (iii) 20 kGy, c, and (iv) 30 kGy, d.

Sample name	Sample code	C_{OX} (farad)	V_{FB} (volt)	$(G/\omega)_{max}$ (farad)	tan δ peak(volt)	$D_{it}\times10^{11}$ ($cm^{-2}\,eV^{-1}$)	Current conduction mechanism
(i) Al/ Al_2O_3/n-Si MOS capacitors	a (group one)	1.98×10^{-10}	1.66	1.37×10^{-9}	-3.03	1.25	Poole–Frenkel
(ii) Al/Al_2O_3/n-Si MOS capacitors irradiated with 10 kGy	b (group two)	2.08×10^{-10}	1.39	7.86×10^{-9}	-2.28	6.48	Poole–Frenkel
(iii) Al/Al_2O_3/n-Si MOS capacitors irradiated with 20 kGy	c (group three)	3.66×10^{-10}	1.37	8.45×10^{-9}	-1.30	6.95	Poole–Frenkel
(iv) Al/Al_2O_3/n-Si MOS capacitors irradiated with 30 kGy	d (group four)	4.03×10^{-10}	1.16	1.42×10^{-8}	-1.12	11.58	Poole–Frenkel

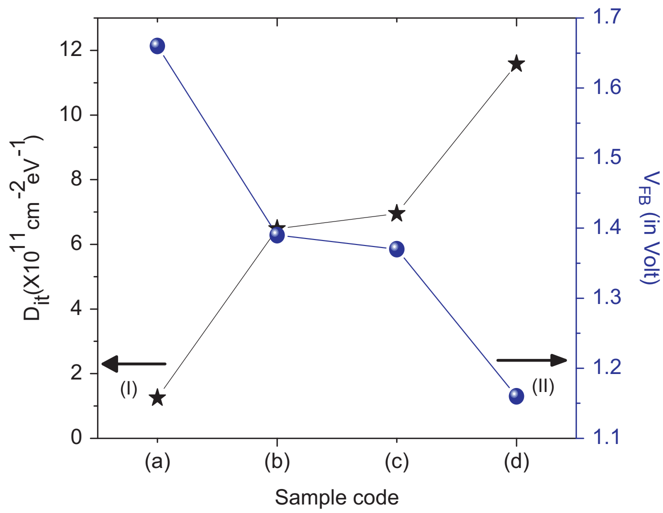

Fig. 5. (I) Flatband voltage (V_{FB}) and (II) D_{it} of Al/Al_2O_3/n-Si MOS capacitors with different electron radiation doses. (i) Zero, a, (ii) 10 kGy, b, (iii) 20 kGy, c, and (iv) 30 kGy, d.

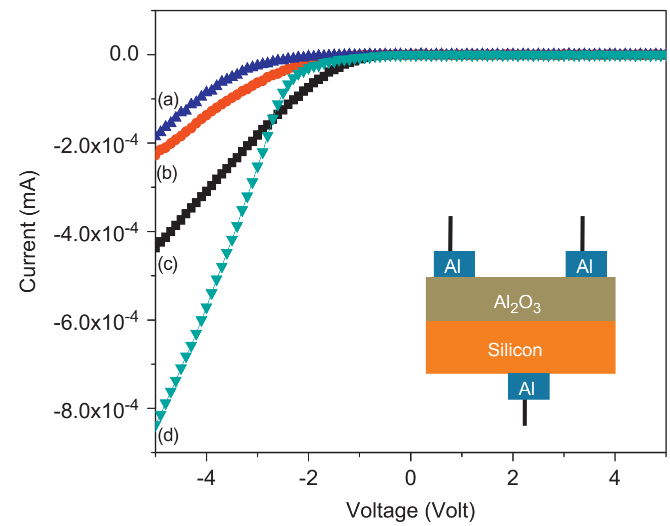

Fig. 7. Leakage current (I)–voltage(V) characteristic of Al/Al_2O_3/n-Si MOS capacitors with different electron radiation doses. (i) Zero, a, (ii) 10 kGy, b, (iii) 20 kGy, c, and (iv) 30 kGy, d, and schematic of the measurement is shown in inset.

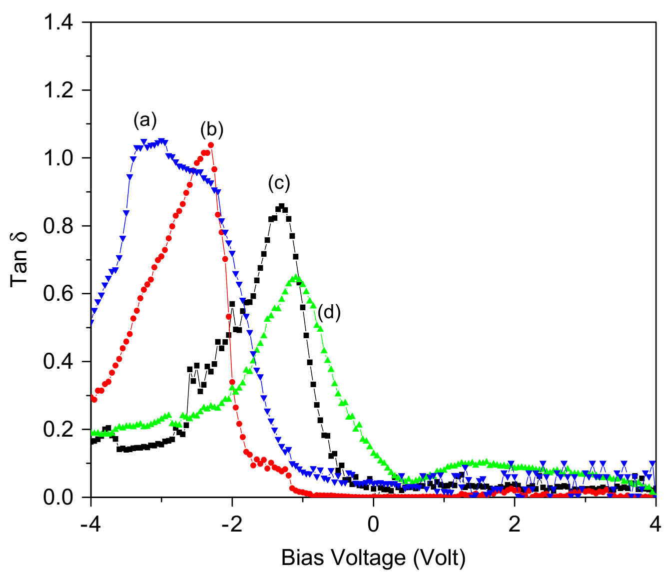

Fig. 6. tan δ of Al/Al_2O_3/n-Si MOS capacitors with different electron radiation doses. (i) Zero, a, (ii) 10 kGy, b, (iii) 20 kGy, c, and (iv) 30 kGy, d.

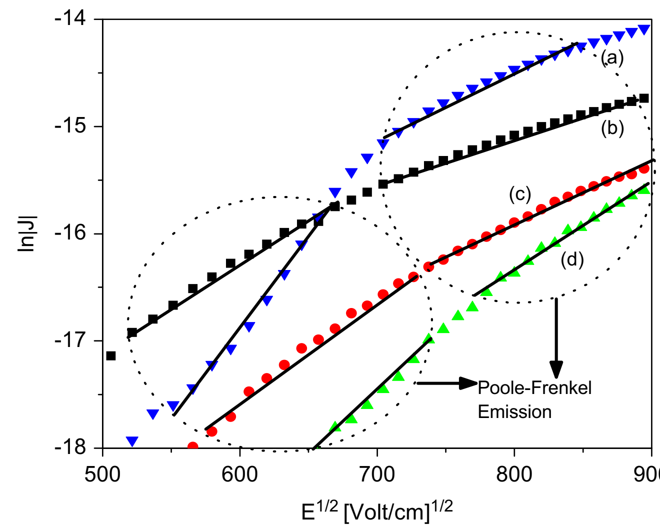

Fig. 8. Plot of the ln $|J|$ vs $\sqrt{E}$ and conduction mechanism of Al/Al_2O_3/n-Si MOS capacitors with different electron radiation doses. (i) Zero, a, (ii) 10 kGy, b, (iii) 20 kGy, c, and (iv) 30 kGy, d.

and (2 3 0) of $Al_2(SiO_4)O$ (JCPDS card No.87-1712), respectively. Peak corresponding to $Al_2(SiO_4)O$ signifies that substrate Si atoms have diffused into the deposited Al_2O_3 film. The increase in the peak intensity of $Al_2(SiO_4)O$ with increasing electron dose implies occurrence of higher inter-diffusion and recrystalization at the Al_2O_3–Si interface. The 6 MeV electrons transferred the energy to the lattice point causing local heating and generating high temperature.

Fig. 3 represents the C–V characteristics of samples a–d. It shows that the capacitance of all irradiated samples increases with increasing electron dose at accumulation region. The increase of the capacitance at accumulation region with electron dose may be caused by two reasons, (i) variations in dielectric properties of the oxide layer and (ii) charge trapping which generates the dangling bonds at the interface of the films. The high energetic electrons produce defects in the samples, which may cause the variation in dielectric properties. Furthermore, the high energy electron also create a large number of electron–hole pairs along the path (Tataroğlu et al., 2007), which may cause the charge trapping in the samples. A parallel shift of the depletion region in all the irradiated samples towards the negative voltage side with respect to electron dose was observed. The shifting of depletion region towards the negative bias may be due to hole trapping at the vacancy sites of oxide layer. The increase of electrons dose increases the % of hole trapping at the vacancy site.

Fig. 4 represents the G/ω–V characteristics of samples a–d. The figure shows that the conductance increases with increasing electron dose from sample b to d at accumulation region. It can be explained by the radiation induced conductivity C_r and the dose rate D_r which are related through the expression (Ergin et al., 2010):

$$C_r = \varepsilon k D_r{}^n \quad (1)$$

where k is a constant, $\varepsilon(\varepsilon_0\varepsilon_r)$ is the dielectric constant of the oxides, and the exponent n is energy distribution of the radiation induced traps in the oxide layers. Eq. (1) implies that the conductivity, C_r increases with increasing dose rate D_r. This equation is well in agreement with that we observed conductance increases with increasing electron dose from sample b to d. The conductivity in oxides is governed mostly by the mechanism of hopping charge carriers. The number of sites available for hopping increases with electron doses. The relation between the mobility and dose rate is given by

$$\mu = (\text{const})D_r^{2\Delta-1} \tag{2}$$

where, Δ=exponent for dose rate (Thangadurai et al.,2009). Eq. (2) is also well in agreement with our results. The high energy electrons generate the dangling bonds and defects at the interface, which may cause the conductance of the MOS structure (Gökçen et al., 2008).

Fig. 5 (I) shows significant changes in flat band voltage of the samples a–d. Flat band capacitances (C_{FB}) were calculated using the equation,

$$C_{FB} = \frac{(C_{OX} \cdot C_{SFB})}{(C_{OX} + C_{SFB})}$$

where C_{SFB} is the depletion layer capacitance, C_{OX} is maximum value of the capacitance, C_{FB} corresponding voltage is flat band voltage (V_{FB}). It shows that flat band voltage decreases with increasing electron dose from sample (b) to (d). The higher electrons doses induce excess electron holes forming more positive charge in the transition layer. These extra charges cause the shifting of flat band voltage ΔV_{FB} as well as depletion region. This shift, which is always seen in the negative direction, is generally attributed to trapping of holes generated by radiation. This causes shifting of the depletion region towards the negative voltage observed in Fig. 3 (Ergin et al., 2010). The flat band voltage of irradiated Al/Al_2O_3/n-Si capacitors varied from 1.66 to 1.16 V. Soliman et al. (1995) reported the variations in flat band voltage of Al_2O_3/p-Si from 1.2 to 1.6 V with the variations of gamma dose up to 50 krad.

Fig. 5(II) shows D_{it} of the samples a–d. The interface trap density D_{it} was estimated by Hill–Coleman method (Hill and Coleman, 1980). The oxide layer of MOS capacitor gets two types of interface layers, one with the top metal gate and second with the bottom Si substrate. These interface layers are widely different due to the thermodynamic instability of these oxide materials with Si and metal. Generally, the bottom interface affects the Si channel mobility, while the defects at the metal–insulator interface cause the Fermi level pinning which affects the transistor drive current changes. Furthermore, D_{it} also depends on the dangling bonds existing at the interface. The interfacial trap density (D_{it}), interfacial defect capacitance (C_{it}) and dose rate (D_r) are related through the equations (Scofield John et al., 1991; Cheng et al., 2011):

$$C_{it}(f) = q \cdot D_{it} \tag{3}$$

$$D_{it} = \kappa_g \cdot f_y \cdot D_r \cdot t_{OX} \cdot f_{it} \tag{4}$$

where κ_g=number of electron–hole (e–h) pairs produced per unit dose, f_y=probability that an e–h pair escapes recombination, t_{OX}=oxide thickness, D_r=radiation dose rate and f_{it}=number of interface traps created per radiation-induced e–h pair. Fig. 5(II) shows that D_{it} increases with increasing electron dose which was expected from Eq. (4) above. The interfacial defects arise from the inter diffusion atoms, nonstoichiometric cation or anion vacancies and the dangling bonds (Callister et al., 2009). The dangling bond is an unpaired electron and it is the result of an effective mismatch between two layers (Tataroğlu et al., 2007). The electron higher dose may produce more defects via dangling bonds as a result of higher interfacial trap density.

Generally, dipoles are produced in the dielectric, which governs the dielectric properties. The dielectric relaxation can be explained by the following relation:

$$\tan\delta = \frac{2\pi f \tau_0 S_r}{1+(2\pi f \tau_0)^2}$$

where S_r is the relaxation strength, which depends on the concentration of dipoles, τ_0 is the relaxation time for dipole orientation, f is the frequency of the applied electric field and tan δ is the dissipation factor (Alegaonkar et al., 2002). The dielectric relaxations are characterized from a plot of tan δ vs V. Fig. 6 shows the graph of tan δ vs voltage at 500 kHz of the samples a–d. In all the samples a–d, the relaxation loss peaks are broad. This is due to the overlapping of a large number of different relaxation periods of dipoles. The relaxation peak is observed at higher voltage for sample a. This might be due to oscillations of the rigid oxide molecule of the oxide material, under a higher applied electric field. The peaks are shifted towards the lower voltage from sample b to d, which might be due to the interfacial polarization and the defects create in the capacitor during electron irradiations. The peak appearance in the tan δ vs voltage curve is due to matching of hopping frequency with the external voltage. This is popularly known by interfacial polarization as established by Koops model and Maxwell–Wagner model (Wagner, 1913; Maxwell, 1929; Koops, 1951).

Fig. 7 shows the leakage current (I) vs voltage (V) of samples a–d. The figure shows no variation in leakage current towards the +ve bias voltage whereas, the variations were observed towards the –ve bias voltage for all the samples. The threshold voltage is corresponding to initiation leakage current that decreases with increasing electron dose. The threshold voltages of samples a–d are -2.32 V, -2.06 V, -1.4 V and -1.4 V, respectively. The maximum leakage currents are -1.81×10^{-4}, -2.2×10^{-4}, -4.27×10^{-4} mA and -8.35×10^{-4} mA of samples a–d, respectively, observed at -5 V bias volt. Fig. 7 shows no identifiable trend in the leakage current with irradiation dose, implying that the excited traps have only a minor effect on current. However, there is a significant change in threshold voltage for leakage current. It is very difficult to accurately establish the carrier flow mechanisms in MOS capacitors since leakage current is very sensitive due to the presence of local non-uniformities (non-uniform thickness or local defect sites).

The possible mechanism of leakage current has been explored through: Poole–Frenkel emission $J = J_0 \exp\lfloor(\beta_{PF}E^{1/2} - \phi_{PF})/k_BT\rfloor$, Slope $= \beta_{PF}/k_BT$, $\beta_{PF} = 2 \times \beta_{SC}$ where ϕ is the barrier height, $J_0 = \sigma_0 E$ is the low-field current density, k_B=Boltzmann's constant, and T=temperature in Kelvin, β_{SC}=Schottky coefficient. The leakage current mechanism proposed from the plot of ln $|J|$ vs $\sqrt{E}$ of samples a–d are shown in Fig. 8. It shows that the linear behavior of ln $|J|$ vs $\sqrt{E}$. The slopes were used for estimating the experimental "β" values, i.e., ($k_BT \times$ slope). These experimental values of β_{PF} were compared with the theoretical values (Laha et al., 2010) and found the leakage current of samples a–d are due to Poole–Frenkel mechanism. In our previous publication, we proposed the leakage current mechanism for the MOS capacitor of oxide thickness ~50 nm was due to both Schottky and Poole–Frenkel (Laha et al., 2010); however, in the present work, we observed that the leakage current mechanism for the MOS capacitor of oxide thickness ~100 nm is due to only Poole–Frenkel effect. This is due to the higher oxide thickness. Higher oxide thickness needs high field to overcome the potential barrier, hence Schottky type mechanism could not observed in the present work.

4. Conclusions

Laboratory-made Al/Al_2O_3/n-Si MOS capacitors were irradiated with 6 MeV electrons at three different doses. The variations in the electrical parameters such as leakage current, conductance, flat-band voltage, interface trap density, and tan δ of the MOS capacitor with the different electron doses were studied. It was observed that the 6 MeV electron beam caused the variations in crystallinity, defects and dangling bonds at the interface, which eventually results in the variation of electrical properties. The results indicate that the electrical parameters of such MOS capacitors may be customized by energetic electron beam irradiation method.

Acknowledgement

The authors wish to acknowledge BRNS, DAE, Mumbai, India, for funding the project.

References

Alegaonkar, P.S., Bhoraskar, V.N., Balaya, P., Goyal, P.S., 2002. Dielectric properties of 1 MeV electron-irradiated polyimide. Appl. Phys. Lett. 80 (4), 640–642.

Bhuvaneswari, H.B., Reddy Rajagopal, V., Rao Mohan, G., 2006. Electrical characteristics of ZrN metallised metal–oxide–semiconductor and metal–insulator–metal devices. J. Mater. Sci. Mater. Electron. 17, 335–339.

Callister Jr, W.D., Rethwisch David, G., Balasubramanium, R., 2009. Materials Science and Engineering. Wiley India (P) Ltd.

Cheng, Cheng-Wei, Apostolopoulos, G., Fitzgerald Eugene, A., 2011. The effect of interface processing on the distribution of interfacial defect states and the *C–V* characteristics of III–V metal–oxide–semiconductor field effect transistors. J. Appl. Phys. 109, 023714.

Cricchi, J.R., Barbe, D.F., 1971. Compensation of radiation effects by charge transport in metal–nitride–oxide–semiconductor structures. Appl. Phys. Lett. 19, 49–51.

Enge, Harald A., 1972. Introduction to Nuclear Physics. Addison-Wesley Publishing Company.

Ergin, F. Belgin, Turan, Raşit, Shishiyanu, Sergiu T., Yilmaz, Ercan, 2010. Effect of γ-radiation on HfO_2 based MOS capacitor. Nucl. Instrum. Methods Phys. Res. B 268, 1482–1485.

Frederickson, A.R., 1993. Radiation-induced voltage on spacecraft internal surfaces. IEEE Trans. Nucl. Sci. 40 (6), 1547–1554.

García, H., Dueñas, S., Castán, H., Gómez, A., Bailón, L., Barquero, R., Kukli, K., Ritala, M., Leskelä, M., 2009. Irradiation effect on dielectric properties of hafnium and gadolinium oxide gate dielectrics. J. Vac. Sci. Technol., B 271, 416–420.

Garrett, H.B., Whittlesey, A.C., 2000. Spacecraft charging, an update. IEEE Trans. Plasma Sci. 28 (6), 2017–2028.

Gökçen, M., Tataroğlu, A., Altındal, Ş., Bülbül, M.M., 2008. The effect of ^{60}Co (γ-ray) irradiation on the electrical characteristics of Au/SnO_2/n-Si (MIS) structures. Radiat. Phys. Chem. 77, 74–78.

Hill, W.A., Coleman, C.C., 1980. A single frequency approximation for interface state density determination. Solid-State Electron. 23 (9), 987–993.

Hughes, H.L., Benedetto, J.M., 2003. Radiation effects and hardening of MOS technology: devices and circuits. IEEE Trans. Nucl. Sci. 50 (3), 500–521.

Kim, H.S., Kim, Yongmin, Noh, S.J., Kim, M.H., 2004. Total ionizing dose effects in MOS devices for different radiation sources. J. Korean Phys. Soc. 45, S820–S823.

Koops, C.G., 1951. On the dispersion of resistivity and dielectric constant of some semiconductors at audio frequencies. Phys. Rev. 83, 121.

Laha, Pinaki, Panda, A.B., Dahiwale, S., Date, K., Patil, K.R., Barhai, P.K., Das, A.K., Banerjee, I., Mahapatra, S.K., 2010. Effect of leakage current and dielectric constant on single and double layer oxides in MOS structure. Thin Solid Films 519, 1530–1535.

Maxwell, J.C., 1929. Electricity and Magnetism, 1. Oxford: Oxford University Press.

McKenna-Lawlor, S., Kudela, K., Kecskemdty, K., Chang, S.W., 2003. Spacecraft measurements of ions and electrons ($>$40 keV) near and far upstream of the earth's bow shock. Adv. Space Res. 31, 933.

Popov, G.V., Degtjarev, V.I., Sheshukov, S.S., Johnstone, A.D., 1997. Influence of geostationary spacecraft charging on measurement s of low energy (0.05–20 keV) electron spectra. Adv. Space Res. 20, 449.

Schmidt, P.F., Rand, M.J., Mitchell, J.P., Ashner, J.D., 1969. Radiation-insensitive silicon oxynitride films for use in silicon devices. IEEE Trans. Nucl. Sci. NS-, 16211–16219.

Scofield John, H., Trawick, M., Klimecky, P., Fleetwood, D.M., 1991. Corelation between preirradiation channel mobility and radiation induced interface-trap charge in metal–oxide–semiconductor transistors. Appl. Phys. Lett. 58, 2782.

Soliman, F.A.S., Al-Kabbani, A.S.S., Sharshar, K.A.A., Rageh, M.S.I., 1995. Characteristics and radiation effects of MOS capacitors with $A1_2O_3$ layers in p-type silicon. Appl. Radiat. Isot. 46 (5), 355–361.

Tataroğlu, A., Bölükdemir, M.H., Tanır, G., Altındal, S., Bülbül, M.M., 2007. Effects of beta-ray irradiation on the *C–V* and G/ω–V characteristics of Au/SiO_2/n-Si (MOS) structures. Nucl. Instrum. Methods Phys. Res. B 254, 273–277.

Tataroğlu, A., Altındal, Ş., Bölükdemir, M.H., Tanır, G., 2007. Irradiation effect on dielectric properties and electrical conductivity of Au/SiO_2/n-Si (MOS) structures. Nucl. Instrum. Methods Phys. Res. B 264, 73–78.

Thangadurai, P., Kaplan, W.D., Mikhelashvili, V., Eisenstein, G., 2009. The influence of electron-beam irradiation on electrical characteristics of metal–insulator–semiconductor capacitors based on a high-*k* dielectric stack of HfTiSiO(N) and HfTiO(N) layers. Microelectron. Reliab. 49, 716–720.

Tuğluoğlua, N., Altındalb, S., Tataroğlub, A., Karadeniz, S., 2004. Dielectric properties in Au/SnO_2/n-Si (MOS) structures irradiated under ^{60}Co-γ rays. Microelectron. J. 35, 731–738.

Voigt, M., Sokolowski, M., 2004. Electrical properties of thin rf sputtered aluminum oxide films. Mater. Sci. Eng., B 109, 99–103.

Wagner, K.W., 1913. Zur Theorie der Unvolkommenen Dielektrika. Ann Physik Bd 40, 817–855.

Winokur, P.S., Schwank, J.R., McWhorter, P.J., Dressendorfer, P.V., Turpin, D.C., 1984. Correlating the radiation response of MOS capacitors and transistors. IEEE Trans. Nucl. Sci. NS-31, 1453–1460.

Xuan, Y., Lin, H.C., Ye, P.D., Wilk, G.D., 2006. Capacitance–voltage studies on enhancement-mode InGaAs metaloxide–semiconductor field-effect transistor using atomic-layer-deposited Al_2O_3 gate dielectric. Appl. Phys. Lett. 88, 263518.